EXHIBIT 5

Harvard Medical School

Harvard TH Chan School of Public Health

John J. Godleski, M.D.
Professor of Pathology Emeritus

Department of Environmental Health (MIPS Program)

jgodlesk@hsph.harvard.edu
Phone (617) 698-5970
Cell (617) 840-9679

June 24, 2021

David Dearing. ESQ
Beasley Allen Law Firm
218 Commerce Street
Montgomery, AL 36104

Re: Tamara Newsome

Dear Mr. Dearing:

I was on the faculty of Harvard Medical School (HMS), Brigham and Women's Hospital (BWH), and Harvard School of Public Health (HSPH) from 1978-2017, retiring as Professor of Pathology in 2017. I graduated from the University of Pittsburgh School of Medicine. As a student, I did research in the Pathology Department learning electron microscopy. In my senior year, I received the top award for research done by a medical student in the United States given by the Student American Medical Association, and published several papers describing that research. I then did an internship and residency in Pathology at the Massachusetts General Hospital, a major teaching hospital of Harvard Medical School. I received further training at HSPH and the University of North Carolina. I was board certified in Anatomic Pathology in 1975. I spent 5 years on the faculty of Medical College of Pennsylvania in Philadelphia in the Department of Pathology where I was in charge of the electron microscopy facility and the autopsy service, and then was recruited to head Pulmonary Pathology at BWH in Boston, a position I held for 37 years. I published more than one hundred and seventy peer-reviewed papers related to pulmonary/environmental pathology including a number using analytical electron microscopy. Notably, I have been senior author on a number of papers using analytical electron microscopy with both X-ray analysis and electron energy loss spectroscopy. In my career, I received more than $30 million in research grants from NIH, EPA, and other funding agencies as Principal Investigator; I led the Particles Research Core in the Harvard-NIEHS Environmental Research Center and I was Associate Director of the Harvard Clean Air Research Center supported by the US EPA. In my daily activities, I was a member of the Pulmonary Pathology and Autopsy Services at Brigham and Women's Hospital. I taught Pathology residents and fellows, medical students, graduate students, and postdoctoral fellows, and I carried out research in my laboratory at HSPH. I was responsible for accurate pathological diagnoses at BWH and I oversaw a research group of as many as 15 people at HSPH. I was the pathologist providing the final opinion on difficult diagnostic cases of lung disease within our department, and I was a recognized expert whose opinion was sought by pathologists from other hospitals in the diagnosis of foreign material in tissues throughout the body using scanning electron microscopy (SEM) and energy dispersive X-ray analyses (EDS). Although now retired, I have full access to laboratory and electron microscopy facilities.

I have recently published six papers regarding talc and tissue pathology (references 1-6). The first paper used tissue digestive procedures and SEM/EDS to quantify talc in lymph nodes in comparison to the use of *in situ* SEM/EDS; the second described the migration and detection of talc in pelvic tissues from the perineum in a series of exposed patients who also had ovarian malignancy. The third concerned the use of spectroscopic magnesium and silicon weight % ratio standards to diagnose talc in human tissues, and the expected

mathematical distribution for such measurements. Three other publications also pertain to talc identification in tissue and resultant pathology (references 4-6).

I have reviewed 31 out of a possible 31 slides on Tamara Newsome (S15-2514), which represent the tissues from the patient's surgical procedure on 3/23/2015 which included hysterectomy, bilateral salpingo-oophorectomy, omentectomy, and right pelvic lymph node excision. Slides on this case were received with the following sublabels: A1-A21 (hysterectomy and bilateral salpingo-oophorectomy;B1-B9 (omentum), and C1 (right pelvic lymph node). All slides were prepared by the Department of Pathology at Holy Cross Health, Silver Spring, Maryland 20910. The histologic slides listed above were reviewed with light microscopy, and the diagnosis of endometrioid carcinoma of the ovary was confirmed. In the surgical pathology report, the tumor was described as being in the right ovary and having a maximum dimension of 10.4 cm, with involvement of the uterine serosa, and without involvement of the left ovary or either fallopian tube. The tumor stage was given in the report as pT2a. No lymphoid tissue was identified in the right pelvic node excision (only fibroadipose tissue was present), thus leaving the lymph node staging at pNX.

The 31 histologic slides on case SP16-53498 were also reviewed using polarized light microscopy, as a means to highlight and detect birefringent foreign material in the same plane of focus with the tissues. Birefringent particle(s) were observed in 8 of the 31 slides reviewed. **Figure 1** illustrates key microscopic findings. In the top photographs within that figure are shown typical areas of the patient's endometrioid carcinoma. In the bottom two photos are shown birefringent particles (highlighted by polarized light microscopy) in the plane of focus with the tissues, within the right ovary.

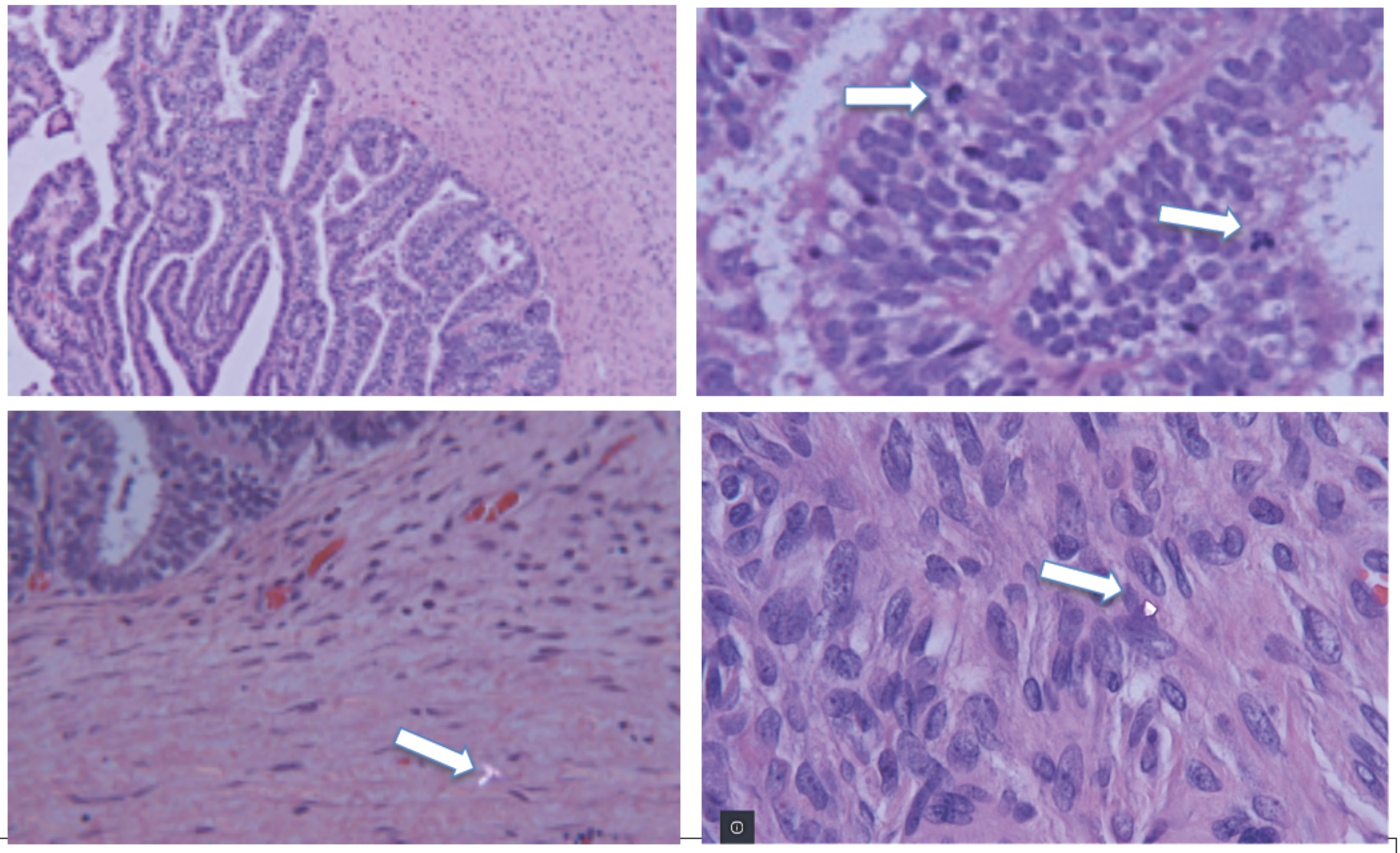

Figure 1. Top Left. Low-power microscopic view of her endometrioid carcinoma of the ovary, with associated fibrous stroma on the right. The tumor shows a distinctly glandular architecture. Original magnification 60x. **Top Right.** High-power view of her endometrioid carcinoma, showing moderate nuclear pleomorphism, a generally columnar cellular architecture, and scattered mitotic figures (arrows). Original magnification 400x. **Bottom left.** A birefringent particle is present within dense collagenous stroma (see arrow) in the plane of focus with the tissues. Ovarian tumor glands are at top left. Original magnification 160x. **Bottom right**. Densely cellular ovarian stroma containing a birefringent particle (see arrow) in the plane of focus with the tissues. Original magnification 400x. All sections stained with hematoxylin-eosin; the bottom two photos are with polarized light microscopy.

Our past experience and the medical literature on the diagnosis of talc in tissues (see references) indicate that the number of birefringent particles in histological sections is robustly correlated with the number of talc particles found by SEM/EDS, since talc is a strongly birefringent material. Also, talc is more likely to be subsequently found by SEM/EDS in tissue sections where 1) the number of birefringent particles by polarized light microscopy is greatest, and 2) the anatomic location of the tissues is most consistent with the expected migration or dissemination patterns for the talc, given its initial application/exposure site (references 1-2).

Taking these factors into consideration, we recommended that five paraffin tissue blocks from Ms. Newsome's 3/23/2015 surgery (A3, A4, A15, A16, A19), respectively representing cervix (A3), uterus (A4), right ovary (A15), right fallopian tube (A16), and left ovary (A19) be obtained for further studies. All five of these paraffin tissue blocks were received and studied as per the *in situ* scanning electron microscopy technique using variable pressure as described by Abraham and Thakral (2007, reference 6), in which the paraffin block may be studied directly in the scanning microscope chamber. The blocks were handled with our standard protocol to prevent contamination of the blocks in our laboratory. This protocol begins with the handling of the blocks using powder-free gloves on pre-cleaned surfaces. The blocks were then sectioned, removing ~50 micrometers of tissue and paraffin using a rotary microtome with a new, stainless steel blade. This sectioning was done to remove any surface contamination from previous storage and handling. After the fresh surface is exposed, the blocks were placed in a pre-cleaned covered container to prevent air particulate contamination, and then transferred to the Electron Microscopy Laboratory. There, blocks were again handled with particle-free gloves on pre-cleaned surfaces, and the blocks were washed in distilled deionized water for ≥2 minutes to remove soluble surface materials such as sodium chloride and sodium phosphate used in processing for histology. When not being examined in the SEM chamber, the blocks were always maintained in closed plastic stub container boxes to provide secure storage and to obviate lab contamination. An example of a paraffin block studied in this case is shown in **Figure 2.**

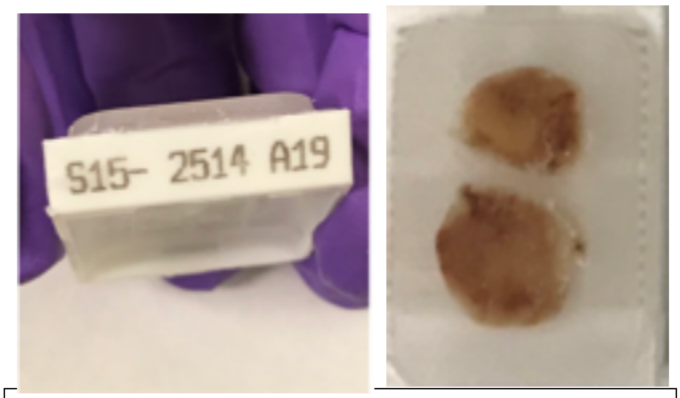

Figure 2. One of the blocks (A19, left ovary) examined by SEM/EDS in this case. **Left:** The labeling (identification) for the block, which is on the side of the cassette. **Right:** Picture of the cut tissue surface of the block (examined by SEM/EDS).

Tissue surfaces were studied with a Hitachi SU6600 field emission SEM with an Oxford EDS, with Oxford instrument software being Aztec 4.1 SP1. EDS detector model was X-Max 50 SDD. The backscatter mode of the microscope was used to highlight mineral particles within the tissue resulting from atomic number contrast. Areas of tissue in the sectioned block surfaces were examined with a systematic rastering technique involving sequential fields at relatively low magnification 200-500x, then when particles were seen, higher magnification was used to show morphological characteristics and to do spectral analysis. In this study, images of backscattered or secondary electrons were acquired using 15 kV accelerating voltage, 10 mm working distance, small beam spot, aperture #1, and 60 Pa vacuum (VP-SEM mode). EDS signals were acquired in either the spot analysis or mapping mode, with dead time <20% and signal counts ~3000-5000 cps. Electron beam penetration depth under the conditions used is estimated to be 2.5 micrometers. Image files were named after the number of EDS site ID, which was consecutive from 1. Spectrum ID was also serial coded consecutively from 1. Once the images or spectra are acquired, the assigned serial ID cannot be changed or replaced.

In studying the blocks of Ms. Newsome by SEM/EDS, a total of 31 talc particles were found in a single ~2-micrometer plane of her tissue blocks (all listed in **Table 1** below). 30 of these were non-fibrous, and one was fibrous, meeting the accepted criteria for a fiber of length: width ratio of ≥3.1 and approximately parallel sides. Approximately half the talc particles (15) were found in block A19 (left ovary). Also in block A19, a small particle with parallel sides and an aspect ratio of 2:1 with a spectrum typical of Tremolite asbestos was found.

This was interpreted as a Tremolite fiber fragment with a Mg/Si atomic weight percent ratio of 0.521 which is within 5% of the accepted Tremolite Mg/Si ratio of 0.541 and including trace amounts of Calcium and Iron. Smaller but still significant numbers of talc particles were distributed across the remaining four blocks (A3, 5 particles; A4, 4 particles; A15, 1 particle; and A16, 6 particles). The 31 talc particles (all in **Table 1** below) that were found all had magnesium and silicon in the EDS spectral proportions for talc, i.e. within ± 5% of the accepted Mg/Si atomic weight % ratio of 0.649.

In the study of the blocks on this case, a total of 821 particles were found and analyzed. Tissues may have carbonaceous material detected in backscattered electron imaging mode by their surface irregularity or other characteristics. Also, in many instances iron, sodium, phosphorus, and calcium may be found in tissues, especially in patients with malignancy. These elements are all considered endogenous to the tissues in this type of study. In the tissues studied of Ms. Newsome, 354 particles had a calcium composition, either with oxygen alone, or in combination with various endogenous elements. Two hundred fifteen (215) particles had a variety of constituents indicative of exogenous materials including 15 non-talc magnesium silicates, 27 magnesium silicates with other cations and/or anions, and 173 other exogenous particles which included various combinations of metals and/or silicon and/or non-metallic elements. The 31 talc particles and fibers (all in **Table 1** below) that were also found in the tissues all had magnesium and silicon in the accepted EDS spectral proportions for talc.

Table 1: Talc block and spectrum numbers and Mg/Si atomic weight % ratios within ± 5% of 0.649

Block/ spectrum #	Mg/Si ratio		Block/ spectrum #	Mg/Si ratio		Block/ spectrum #	Mg/Si ratio
A3 4	0.641		A16 433	0.663		A19 144	0.680
A3 5	0.674		A16 468	0.644		A19 159	0.663
A3 9	0.644		A16 482	0.644		A19 187	0.660
A3 14	0.641		A16 483	0.639		A19 203	0.641
A3 24	0.644		A16 500	0.644		A19 224	0.646
A4 537	0.641		A19 63	0.680		A19 238	0.660
A4 599	0.660		A19 91	0.663		A19 245	0.678
A4 623*	0.680		A19 112	0.622		A19 250	0.650
A4 657	0.636		A19 129	0.617		A19 252	0.669
A15 732	0.660		A19 132	0.650		A19 290	0.620
A16 431	0.678						

*indicates talc fiber spectrum. Aspect ratio for particle A4 623 is ~3.2 :1.

The technique used in the study of Ms. Newsome's tissues examines an extremely small volume of tissue. Comparable studies have been done with asbestos fibers in tissue sections (reference 7), and the finding of one fiber in a tissue section comparable to the amount of tissue studied here would indicate at least 100 fibers per gram of tissue which is indicative of a substantial exposure. If similar approaches were applied to the findings of this study, indications are that very substantial amounts of talc were present in the patient's pelvic tissues. The findings of 31 talc particles spread across 5 out of 5 paraffin tissue blocks by analytical microscopy, using this approach indicates that a significant amount of talc is present within the tissues. In published studies (references 1, 2, 5, 9), significant numbers of talc particles were detected in pelvic tissues in women with ovarian cancer and a history of perineal talc use.

Figure 3 on the following page shows the morphology of two representative talc particles detected in this case, one non-fibrous and the other fibrous, and their EDS spectra (block A19, spectrum 224; block A4, spectrum 623). In both these instances, the atomic weight % ratio of magnesium to silicon is the ratio expected for talc (spectrum 224 = 0.646, spectrum 623 = 0.680, both within ± 5% of the accepted ratio 0.649). The magnesium,

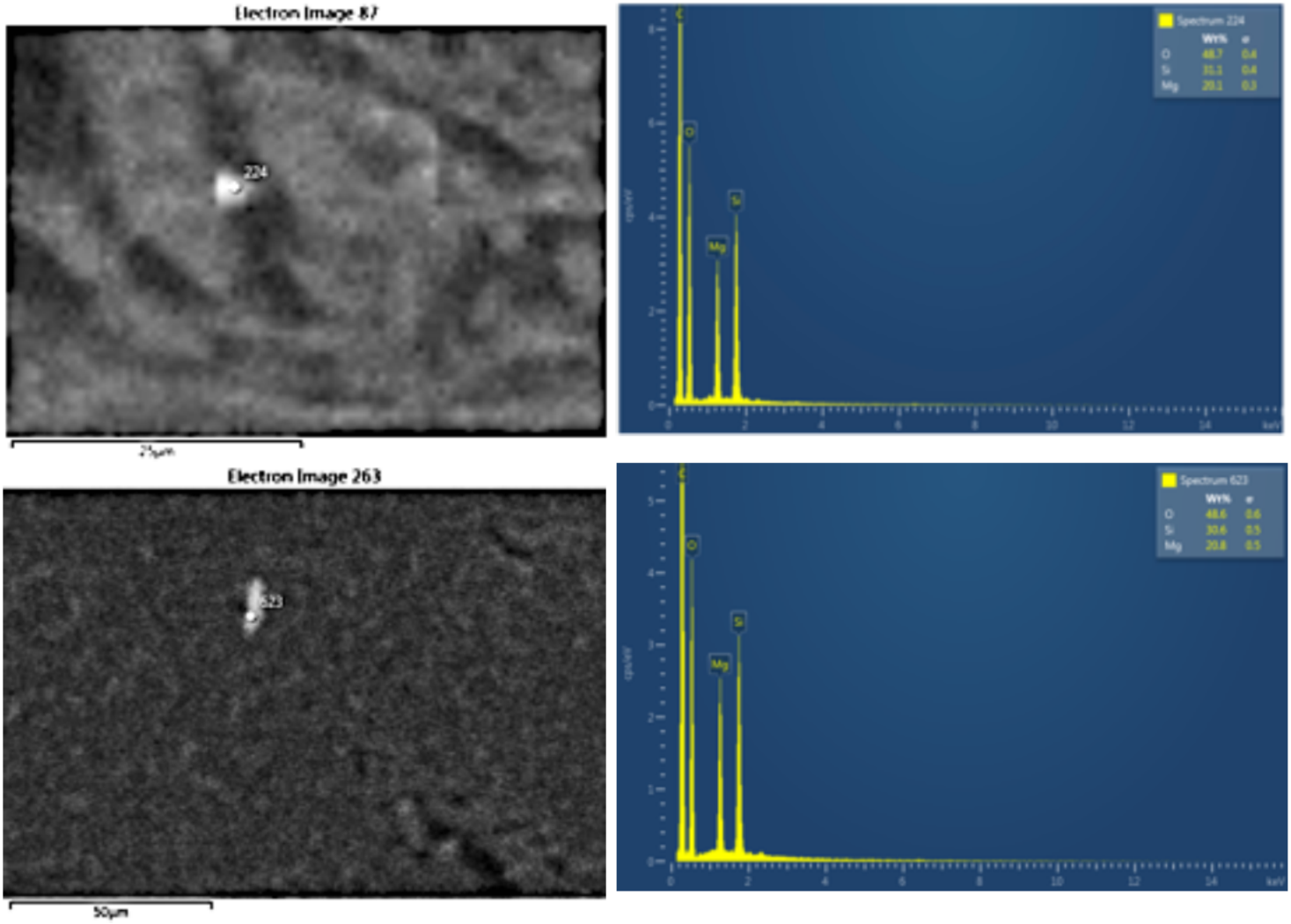

Figure 3. Upper Left. SEM image (87) of a particle in left ovarian tissue (block A19) in backscatter mode. This particle is within tissue and is polygonal and non-fibrous. Using the scale on the photo, the particle is ~4 microns in greatest dimension. **Upper Right**. The EDS spectrum (224) of this particle is shown with magnesium, silicon, and oxygen labeled. Magnesium and silicon have the atomic weight % ratio expected for talc, 0.646 which is within ± 5% of the ratio 0.649. **Lower Left.** SEM image of a fibrous particle in uterus tissue (block A4) in backscatter mode. This particle is within tissue and, using the scale on the photo, has dimensions of ~13 x 4 microns, yielding a length: width ratio of ~3.2 :1. **Lower Right**. The EDS spectrum (623) of this fibrous particle is shown with magnesium, silicon, and oxygen labeled. Magnesium and silicon have the atomic weight % ratio expected for talc, 0.680 which is within ± 5% of the ratio 0.649.

silicon, and oxygen peaks are labeled by the software of the instrument, which is periodically checked to assure that known elemental materials are properly identified.

Figure 4 on the following page shows the Tremolite fiber fragment also found in the tissue of the left ovary in block A19, site 46 electron image 82 and spectrum 215. The finding of this Tremolite fiber fragment by the method used here is highly significant since this form of asbestos is a known contaminant of cosmetic talc and has been shown in recent tissue digestion studies of pelvic tissues to be found in women using talc for personal hygeine. (Reference 10 Steffen et al 2020).

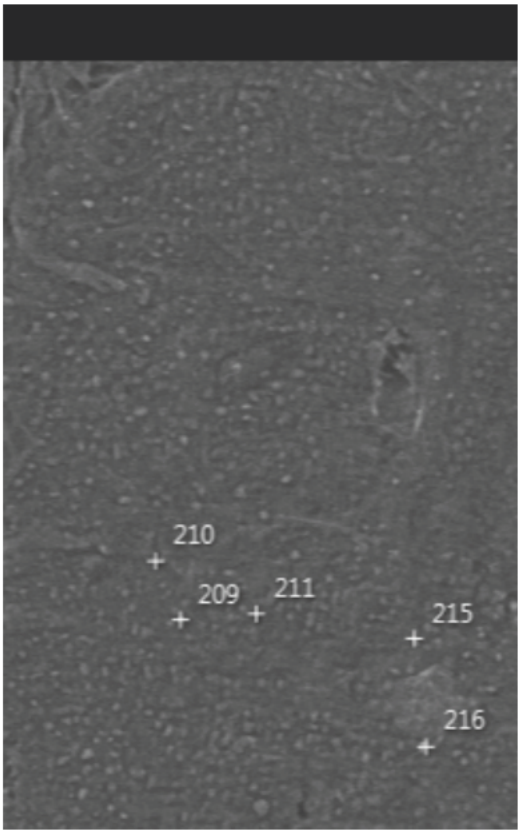
210
209
211
215
216

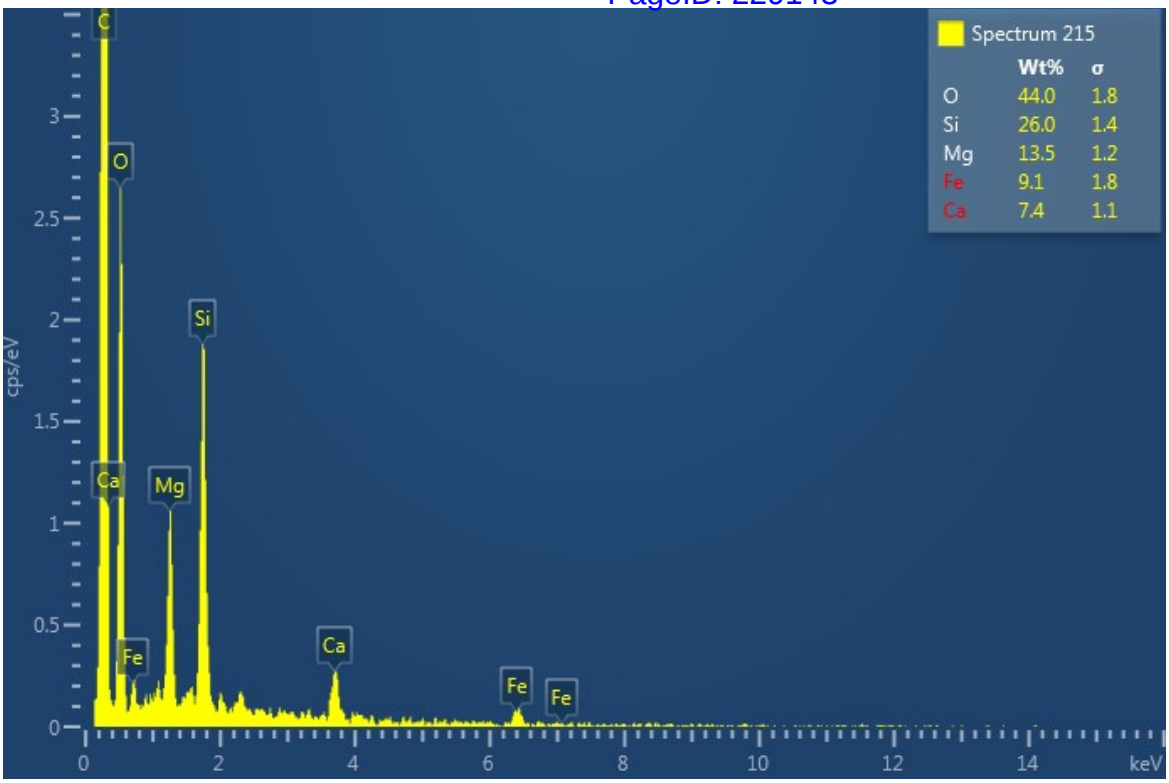

Figure 4 Upper Left SEM image (82) of small particles in left ovarian tissue (block A19) with spectrum numbers, but particles/fibers analyzed obscured by indicator. **Upper Right**. Higher magnification showing particle/fiber morphology, and structure of particle/fiber 215 highlighted with arrow. This structure is within tissue, has parallel sides and a visible aspect ratio of 2:1. Careful inspection of this structure suggests it may in fact have a greater aspect ratio as the lower end appears to disappear into the tissue. **Lower.** Spectrum of particle/fiber fragment 215 showing Mg/Si atomic weight percent ratio of 0.521 which is within 5% of the accepted Tremolite Mg/Si ratio of 0.541 and including trace amounts of Calcium and Iron.

Therefore, based on the findings of this case, it can be stated to a reasonable degree of medical certainty, that the talc and tremolite asbestos found in the tissues of this case are contributory evidence for a causal link between the presence of these materials and the development of this patient's ovarian cancer. All opinions expressed in this report are to a reasonable degree of medical and scientific certainty.

Sincerely,

John J. Godleski, MD

John J. Godleski, MD
Professor Emeritus of Pathology

References:

1. McDonald, SA, Fan Y, Welch, WR, Cramer, DW, Stearns, RC, Sheedy, L, Katler, M, Godleski JJ. Correlative polarizing light and scanning electron microscopy for the assessment of talc in pelvic lymph nodes. Ultrastruct Pathol 43:13-27. 2019. DOI 10.1080/01913123.2019.1593271. PMID: 30898001.

2. McDonald SA, Fan Y, Welch WR, Cramer DW, Godleski JJ. Migration of talc from the perineum to multiple pelvic organ sites: five case studies with correlative light and scanning electron microscopy. Am J Clin Pathol 152: 590-607, 2019. https://doi.org/10.1093/ajcp/aqz080. PMID: 31305893 PMCID: PMC6779257.

3. McDonald SA, Fan Y, Rogers RA, Godleski JJ. Magnesium/silicon atomic weight percent ratio standards for the tissue identification of talc by scanning electron microscopy and energy dispersive X-ray analysis. Ultrastruct Pathol 43: 248-260, 2019. DOI 10.1080/01913123.2019.1692119. PMID: 31736386.

4. Campion A, Smith KJ, Fedulov AV, Gregory DZ, Fan Y, **Godleski JJ**. Identificatio**n** of Foreign Particles in Human Tissues Using Raman Microscopy Analytical Chemistry **2018** *90* (14), 8362-8369 DOI: 10.1021/acs.analchem.8b00271 PMID:29894163

5. Sato E, McDonald SA, Fan Y, Peterson S, Brain JD, Godleski JJ: Analysis of particles from hamster lungs following pulmonary talc exposures: implications for pathogenicity. Part Fibre Toxicol 2020; 17:20. https://doi.org/10.1186/s12989-020-00356-0. PMID: 32498698 PMCID: PMC7271432.

6. Johnson KE, Popratiloff A, Fan Y, McDonald S, Godleski JJ. Analytic comparison of talc in commercially available baby powder and in pelvic tissues resected from ovarian carcinoma patients. Gynecol Oncol 2020; 159: 527-533. PMID: 32977988.

7. Abraham JL, Thakral C. Automated scanning electron microscopy and X-ray microanalysis for in situ quantification of gadolinium deposits in skin. Microscopy 2007; 56: 181-187. PMID: 17951398.

8. Roggli VL, Pratt PC. Numbers of asbestos bodies on iron-stained tissue sections in relation to asbestos body counts in lung tissue digests. Hum Pathol 1983; 14: 355-361. PMID: 6299925.

9. Cramer DW, Welch WR, Berkowitz RS, Godleski JJ. Presence of talc in pelvic lymph nodes of a woman with ovarian cancer and long-term genital exposure to cosmetic talc. Obstet Gynecol 2007; 110: 498-501. PMID: 17666642

10. Steffen JE, Tran T, Yimam M, Clancy KM, Bird TB, Rigler M, Longo W, Egilman DS. Serous Ovarian Cancer Caused by Exposure to Asbestos and Fibrous Talc in Cosmetic Talc Powders-A Case Series. J Occup Environ Med. 2020 Feb;62(2):e65-e77. doi: 10.1097/JOM.0000000000001800. PMID: 31868762.